BERKELEY LAB
Bringing Science Solutions to the World

U.S. DEPARTMENT OF ENERGY
Office of Science

Acceleration of Radiological Mapping by Image Super Resolution

Lei Pan[1], Yen-Chun Liu[2], Simon Mak[2], Jayson R Vavrek[1]

[1]Applied Nuclear Physics Program, Nuclear Science Division, Lawrence Berkeley National Laboratory
[2]Department of Statistical Science, Duke University

Radiation mapping overall goals

Where is the radiation and how bad is it? I.e., what is the radiation *distribution* in the scene?

LiDAR + rad measurements → Scene representation → Rad image reconstruction

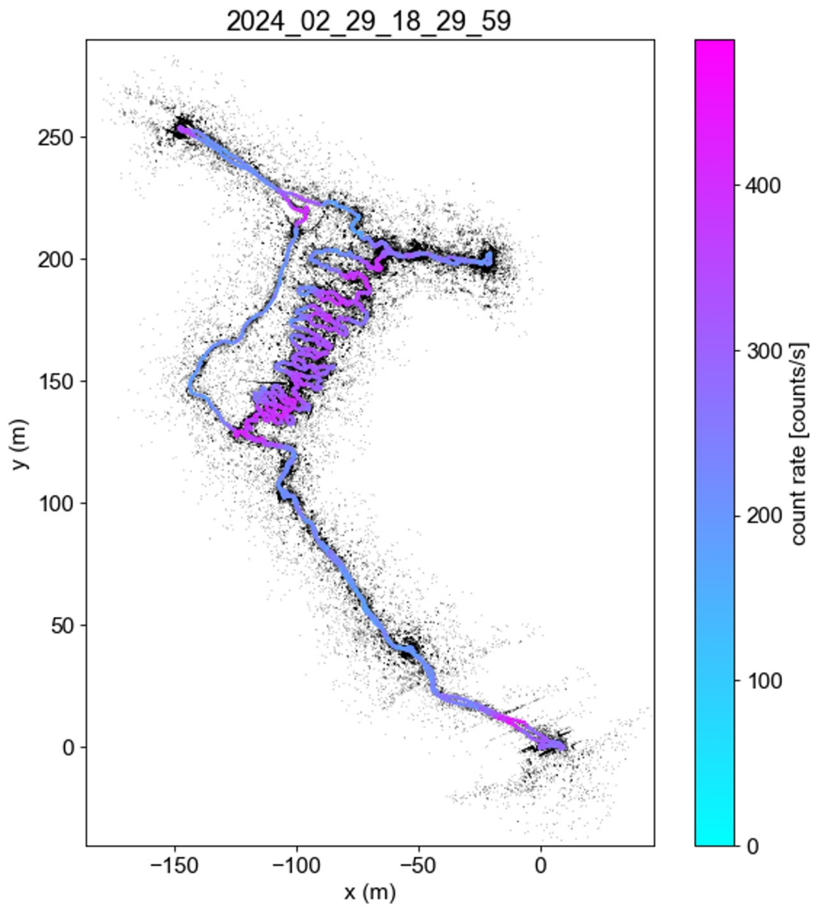

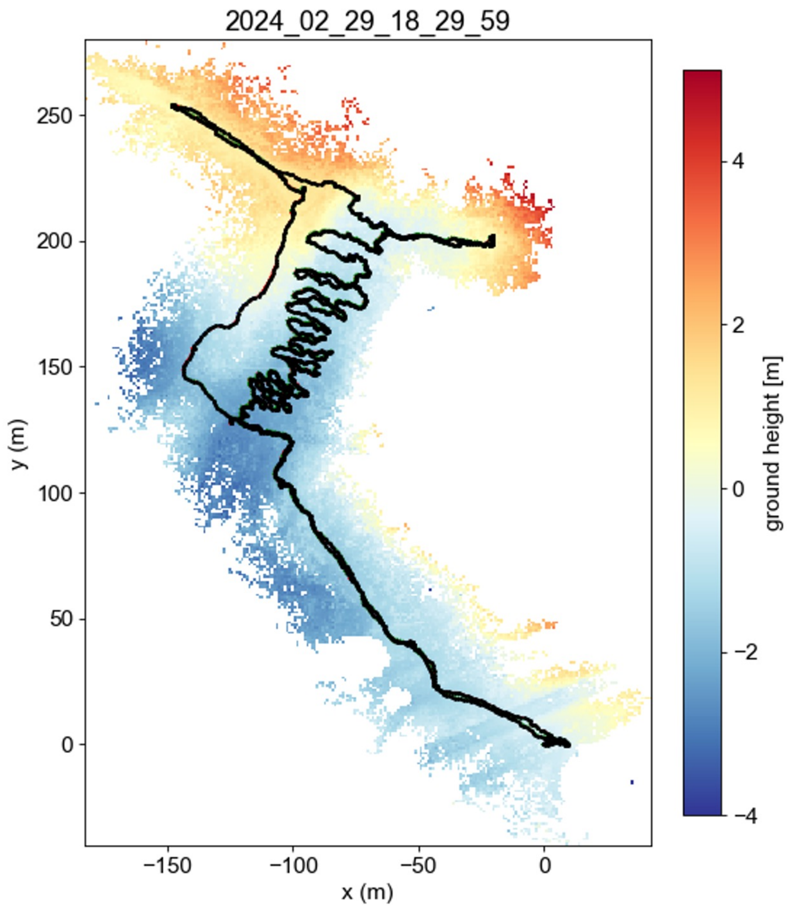

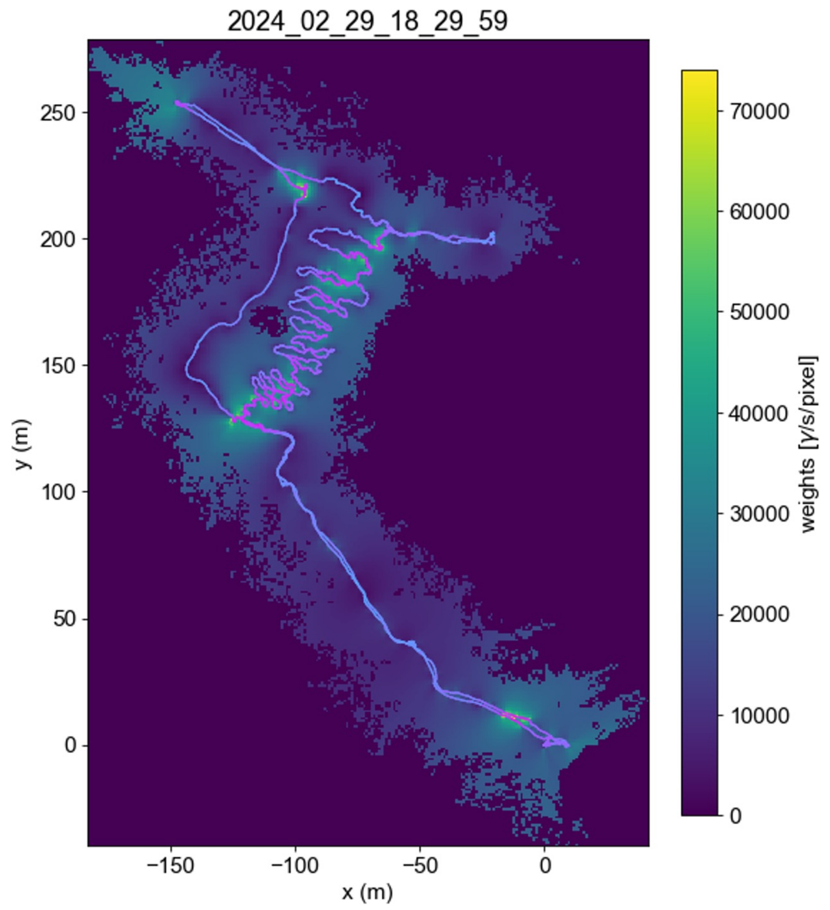

Radiation mapping systems and applications

Handheld / UAS-borne detector systems

Pavlovsky et al. (2019b)

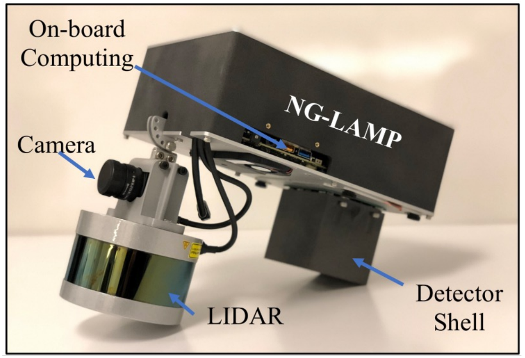

Anisotropic angular efficiency function

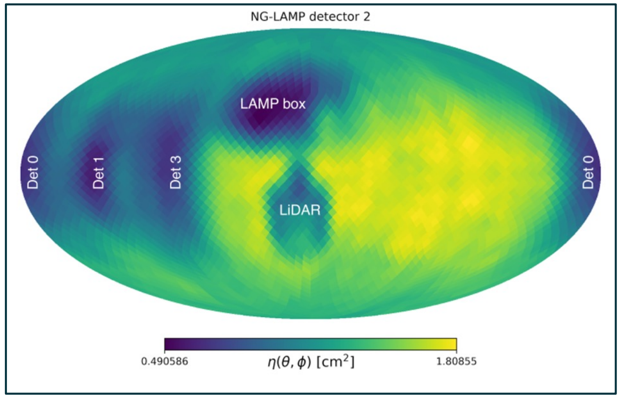

Vavrek et al. (2020)

Contamination mapping / decontamination verification

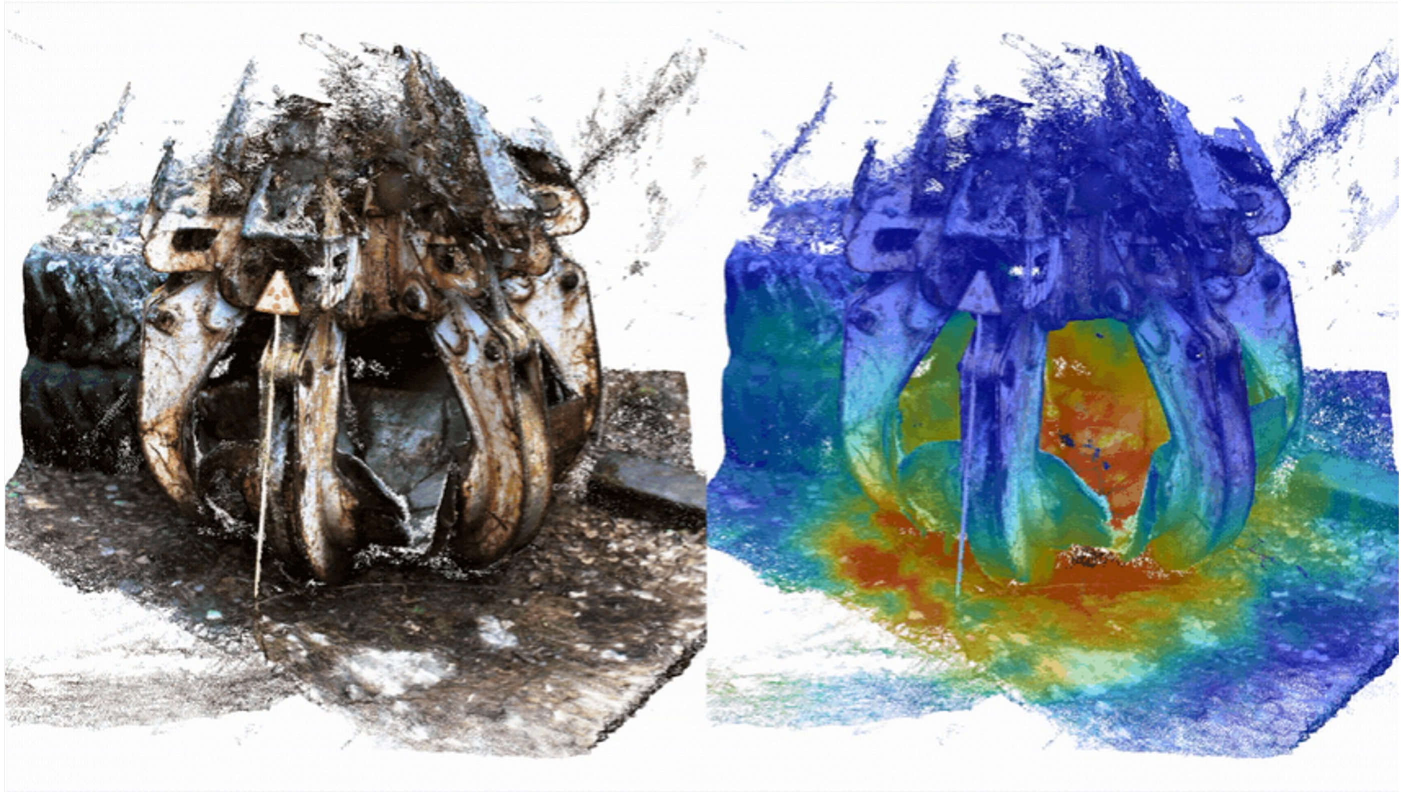

Chornobyl claw, Vetter et al. (2019)

Rad image reconstruction

$$\lambda = V \cdot w + b\, t$$

w: radiation intensity
V: system matrix
b: background count rate
t: measurement time
λ: mean counts

- Measured counts x ~ Poisson(λ)
- Negative log likelihood

$$\ell(\mathbf{x}|\boldsymbol{\lambda}) = [\boldsymbol{\lambda} - \mathbf{x} \odot \log \boldsymbol{\lambda} + \log[\Gamma(\mathbf{x}+1)]]^{\mathrm{T}} \cdot \mathbf{1}$$

- Find the estimates of w and b by minimizing the negative log likelihood

$$\hat{\mathbf{w}}, \hat{b} = \underset{\mathbf{w}, b}{\operatorname{argmin}}\ \ell(\mathbf{x}|\mathbf{w}, b)$$

- Iterative reconstruction algorithm: e.g, Maximum Likelihood Expectation-Maximization (MLEM)

Rad image reconstruction

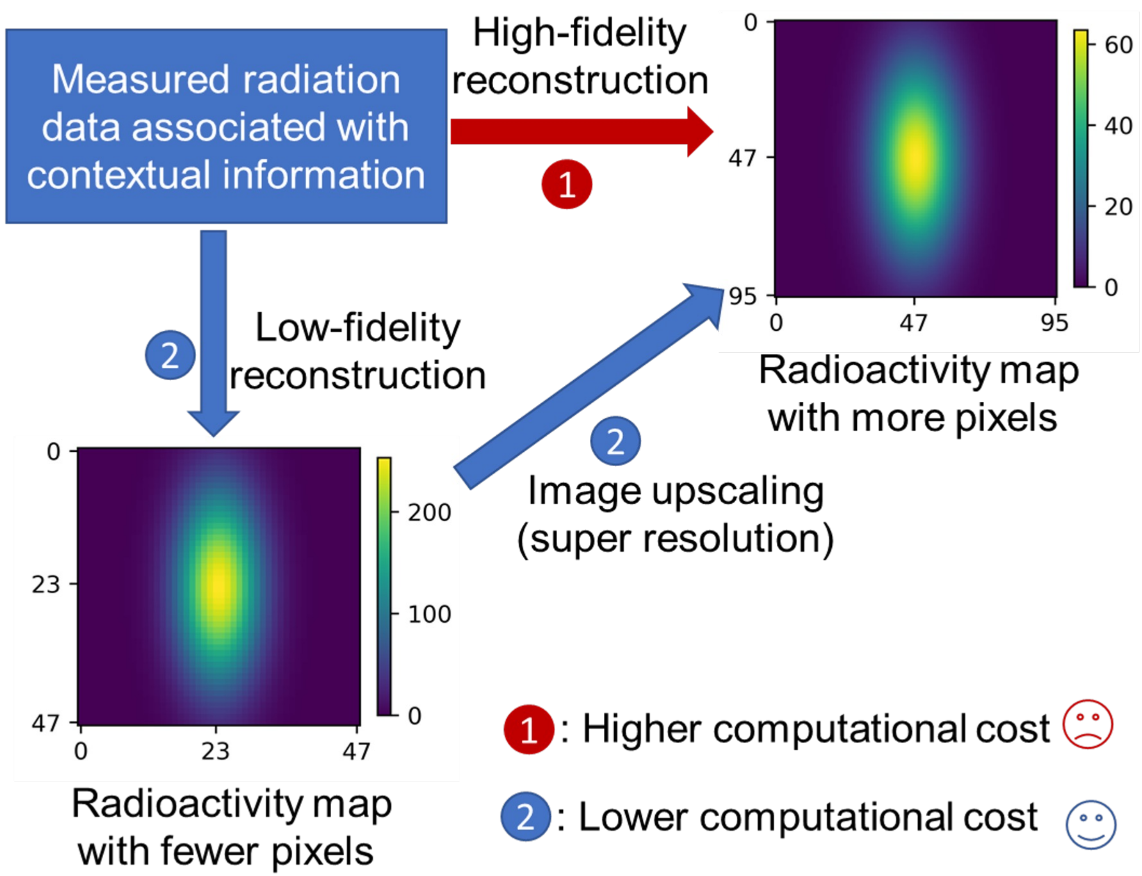

Note: Only 2D map is considered

After low-fidelity reconstruction, perform image upscaling to generate the high-fidelity map

Image upscaling by machine learning algorithms with significantly less computation

Benefits of lower computation cost:

- acceleration of data processing to enable real-time or near real-time reconstruction of high-fidelity results
- reduction of computer memory usage so compact computer can be used on smaller, portable edge systems
  - (can't put an NVIDIA 4090 GPU on every system!)
- reduction of battery usage which allows more system operation time

Image upscaling / Super Resolution (SR) algorithms

Image SR algorithms

Parametric algorithms (learn a fixed set of parameters from training data)
- Convolutional Neural Networks

Non-parametric Bayesian algorithms (complexity change with the data)
- Gaussian Process

Generative Adversarial Networks (GAN) SR

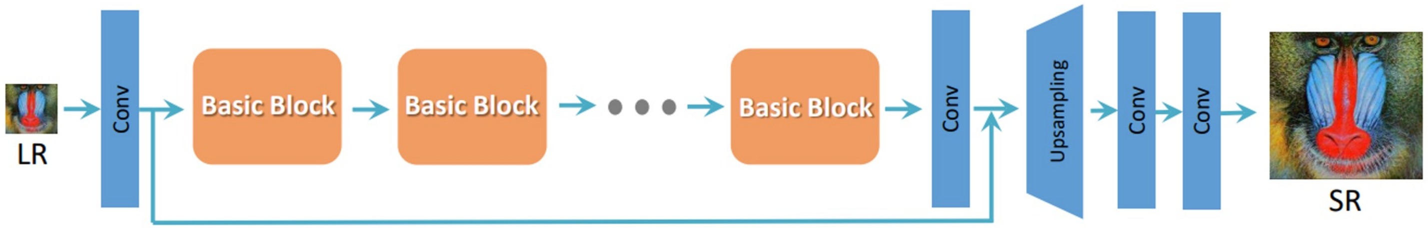

Wang, Xintao, et al *Proceedings of the European conference on computer vision (ECCV) workshops*. 2018.

Single image SR
Gaussian process regression

input output

He, He, and Wan-Chi Siu. *CVPR 2011*. IEEE, 2011.

Channel split convolutional neural network
for thermal image super-resolution

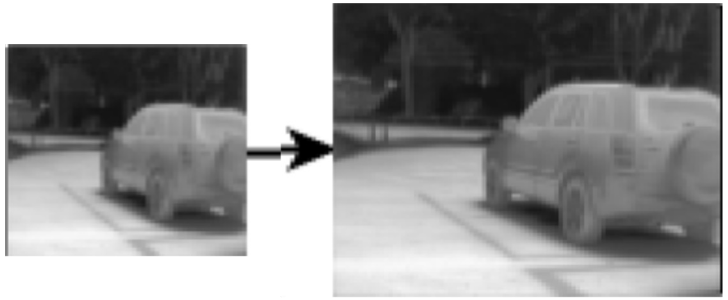

Prajapati, Kalpesh, et al. *Proceedings of the IEEE/CVF Conference on Computer Vision and Pattern Recognition*. 2021.

Image SR applications:
- Computer vision
- Medical imaging
- …
- Radiation map processing

Channel split convolutional neural network (ChaSNet model) for single-channel image SR

Prajapati, Kalpesh, et al. *Proceedings of the IEEE/CVF Conference on Computer Vision and Pattern Recognition*. 2021.
https://github.com/kalpeshjp89/ChasNet.git

Training dataset:
- 3000 image pairs - gaussian ‘elliptical’ *(representative of plumes)*
- 2000 image pairs - gaussian square *(representative of human-made surfaces)*

Synthetic gaussian ‘elliptical’

High resolution (ground truth)

Downsampling

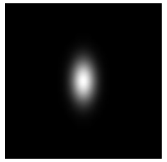

Low resolution

ChaSNet upscaling

Simple upscaling (non - Machine Learning)

- Simple upscaling divide one pixel of low resolution image into 4 pixels
- Each new pixel has intensity 1/4 of the original pixel

Synthetic gaussian square

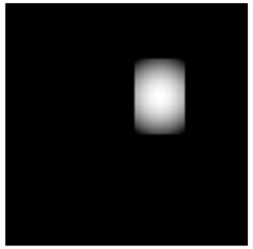

Downsampling

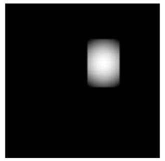

ChaSNet for single channel image SR – performance evaluation

Upscaling performance metrics

- PSNR (Peak Signal-to-Noise Ratio): larger is better
- SSIM (Structural Similarity Index): larger is better, with max 1 for identical images

Results for 10 iterations

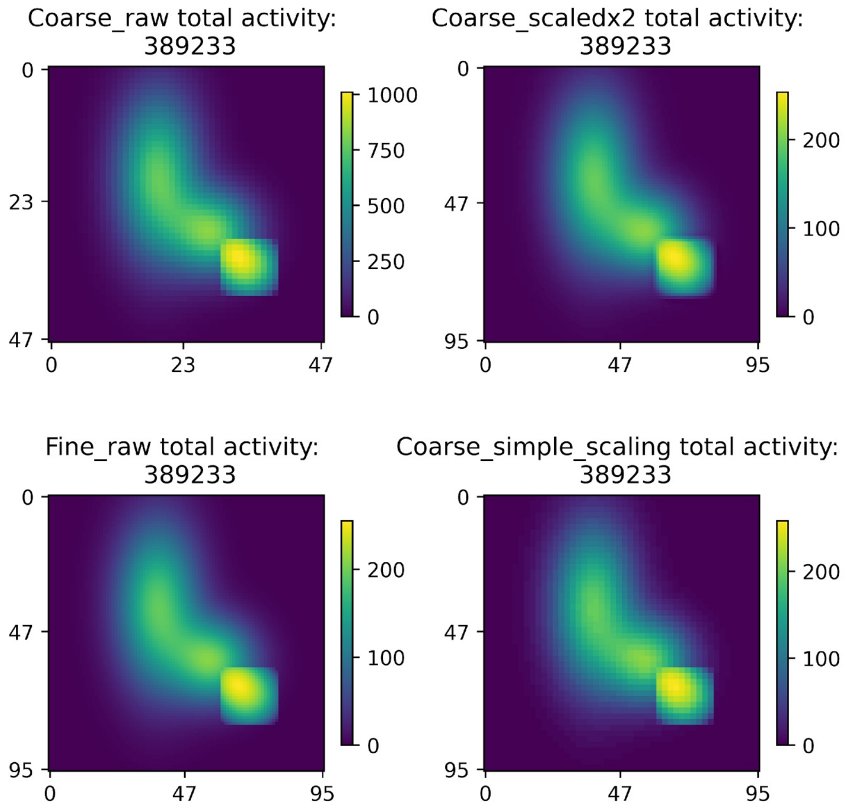

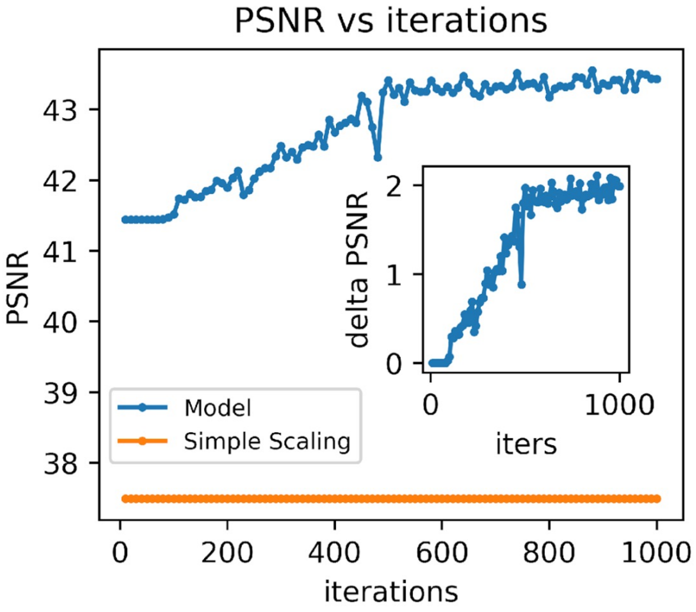

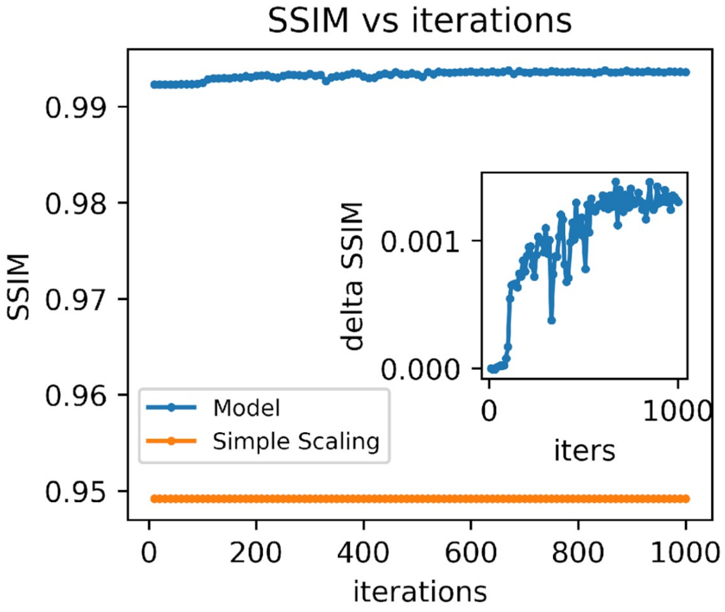

Results for 10 iterations

Percentage Deviation = (upscaled – ground truth) / ground truth * 100%

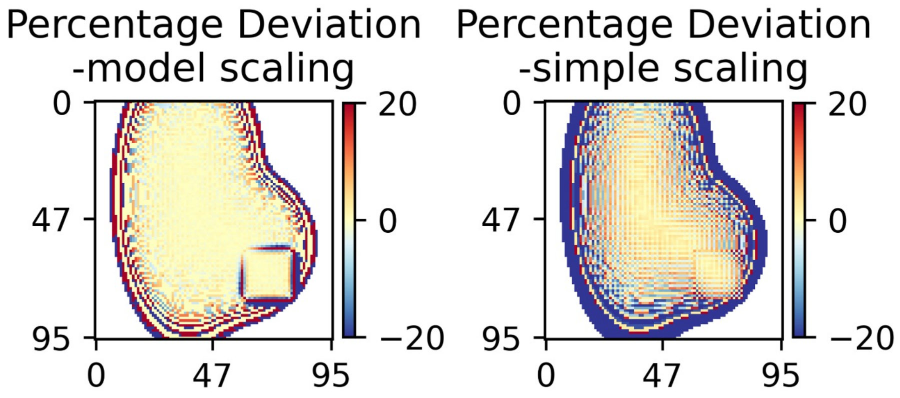

ChaSNet for single channel image SR – advantage for complex patterns

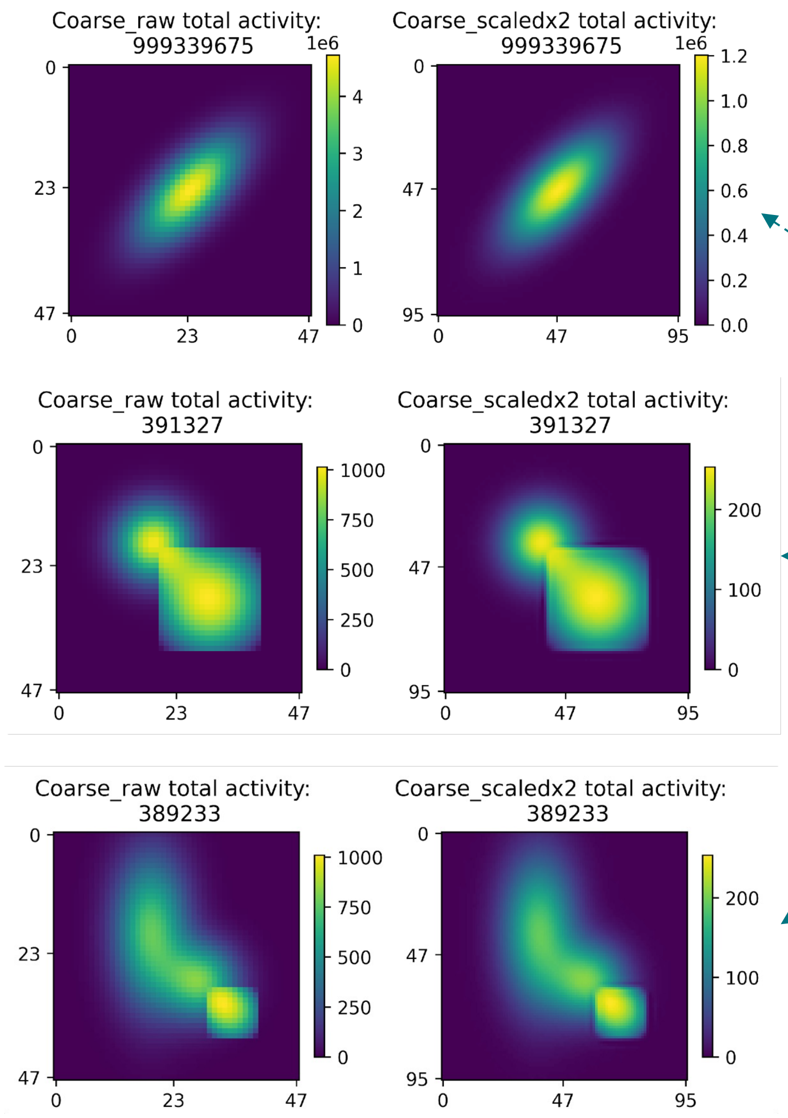

Increase complexity

Patterns	PSNR		SSIM	
	ChaSNet scaling	Simple scaling	**ChaSNet scaling**	Simple scaling
1 elliptical	**50.6**	39.4	**0.990**	0.982
1 elliptical + 1 square	**40.2**	38.0	**0.990**	0.965
2 elliptical + 1 square	**43.6**	37.5	**0.994**	0.949

The ChaSNet model upscaling performs well for complex patterns

Gaussian Process Regression (GPR) model

Under the framework of Gaussian Process Regression, two models, named GPRSR and AGPR, are implemented.

He, He, and Wan-Chi Siu. *CVPR 2011*. IEEE, 2011. https://github.com/fynsta/Super-resolution.git

	GPRSR	AGPR
Training data	single low resolution input image	Dataset with many images
Pre-trained model	No	Yes
Computation speed	Slow for large images	Fast

	PSNR	SSIM
Simple scaling	37.7	0.948
AGPR (100 iterations; arbitrary dataset)	36.0	0.852
GPRSR (50 iterations)	41.9	0.991
ChaSNet	46.1	0.994

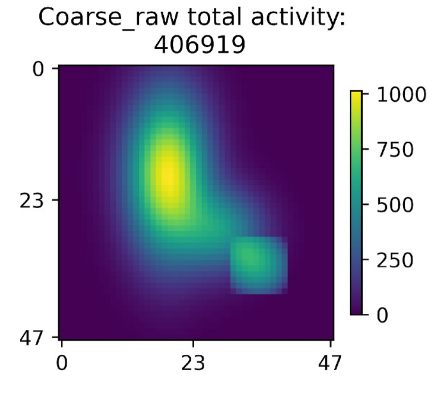

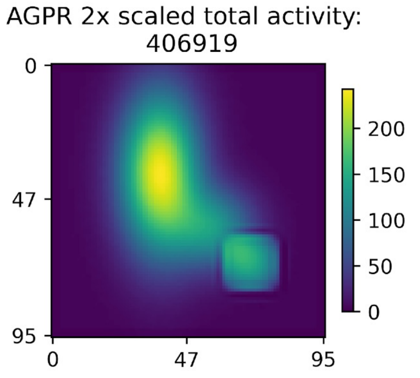

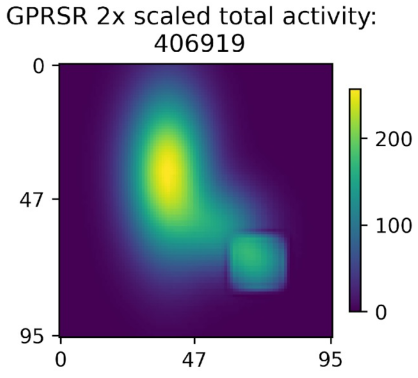

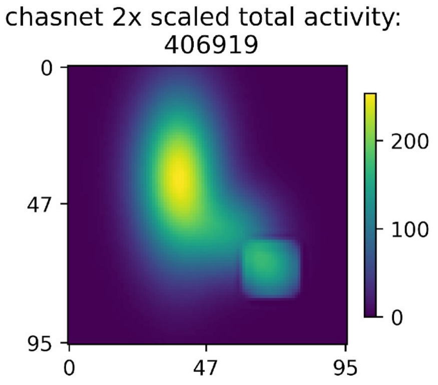

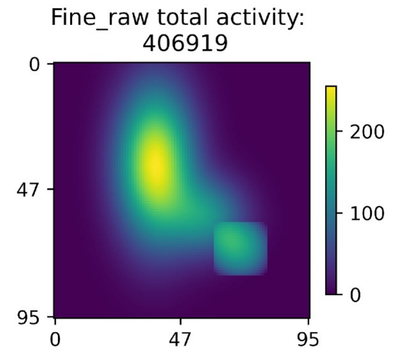

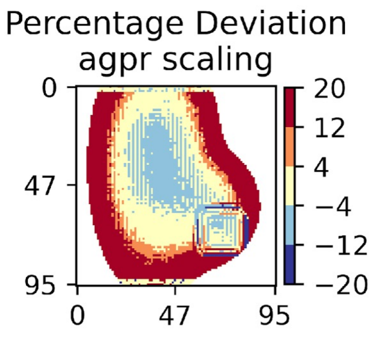

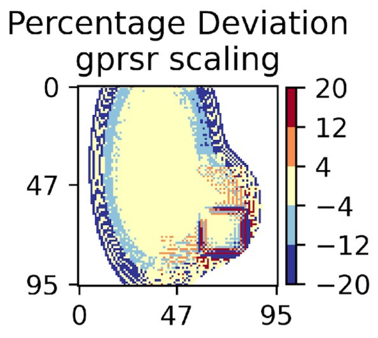

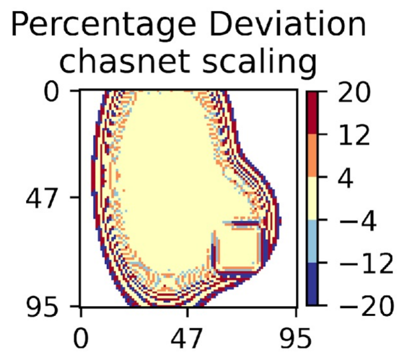

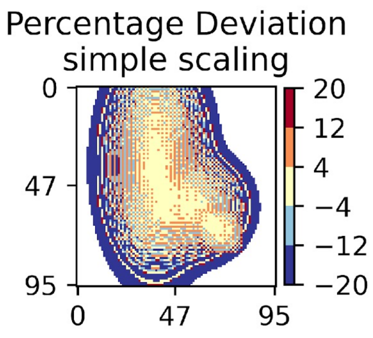

GPR model performance with varied parameters

	Model parameters	PSNR	SSIM
AGPR	arbitrary dataset; 100 iterations	36.0	0.852
	synthetic dataset; 100 iterations	42.9	0.989
	synthetic dataset; 500 iterations	41.7	0.959

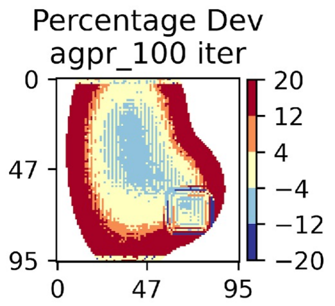

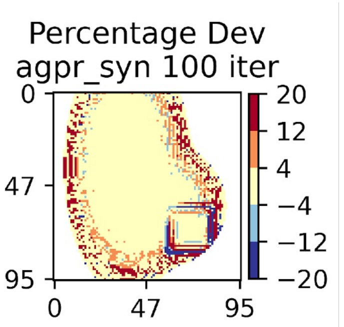

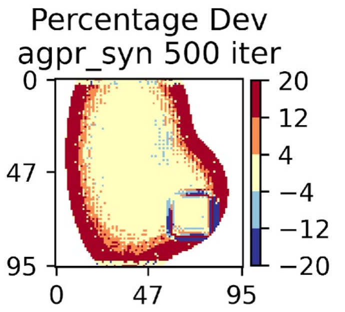

	Model parameters	PSNR	SSIM
GPRSR	50 iterations	41.9	0.991
	500 iterations	42.2	0.990
	5000 iterations	41.9	0.990
ChaSNet		**46.1**	**0.994**

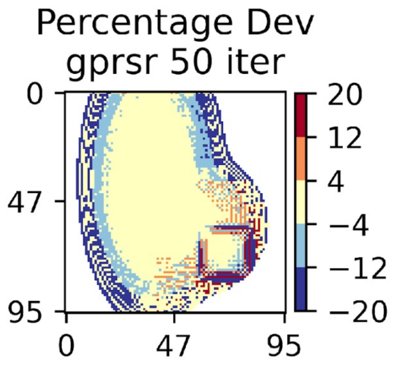

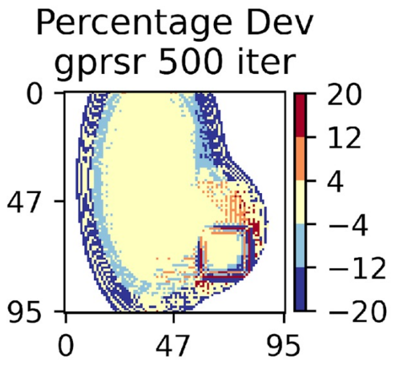

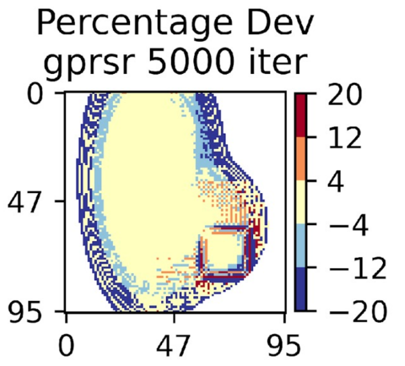

- Optimal performance of GPR models achieved after varying parameters
- **ChaSNet still outperforms the GPR models**

Image inpainting

Image inpainting problem

Ground height map measured by Lidar

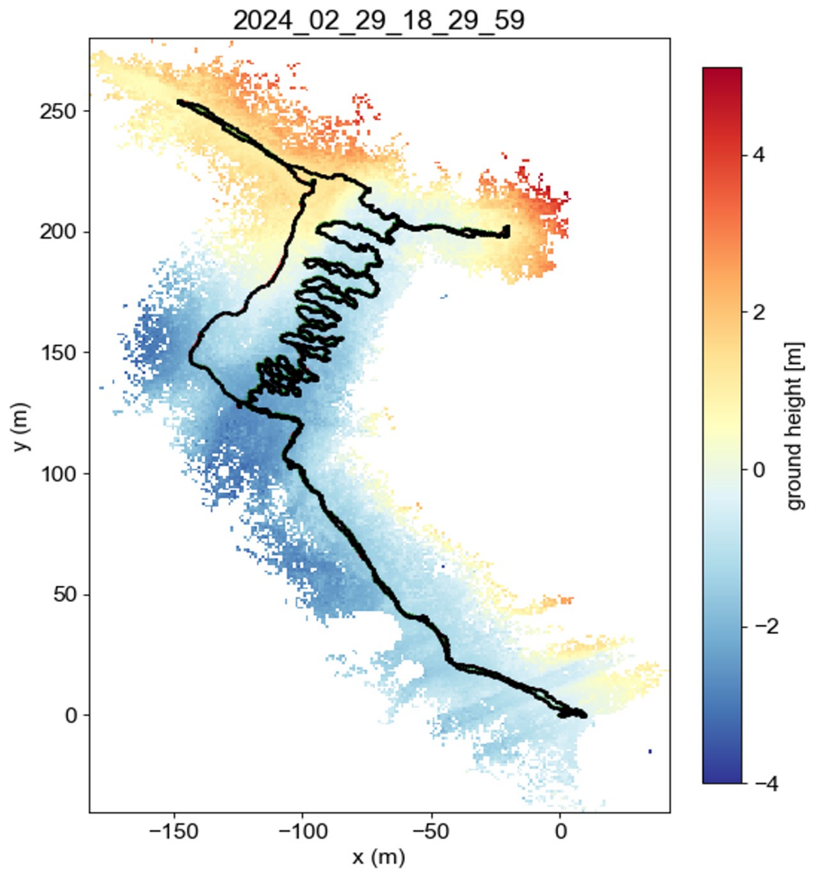

Radiation intensity map reconstructed

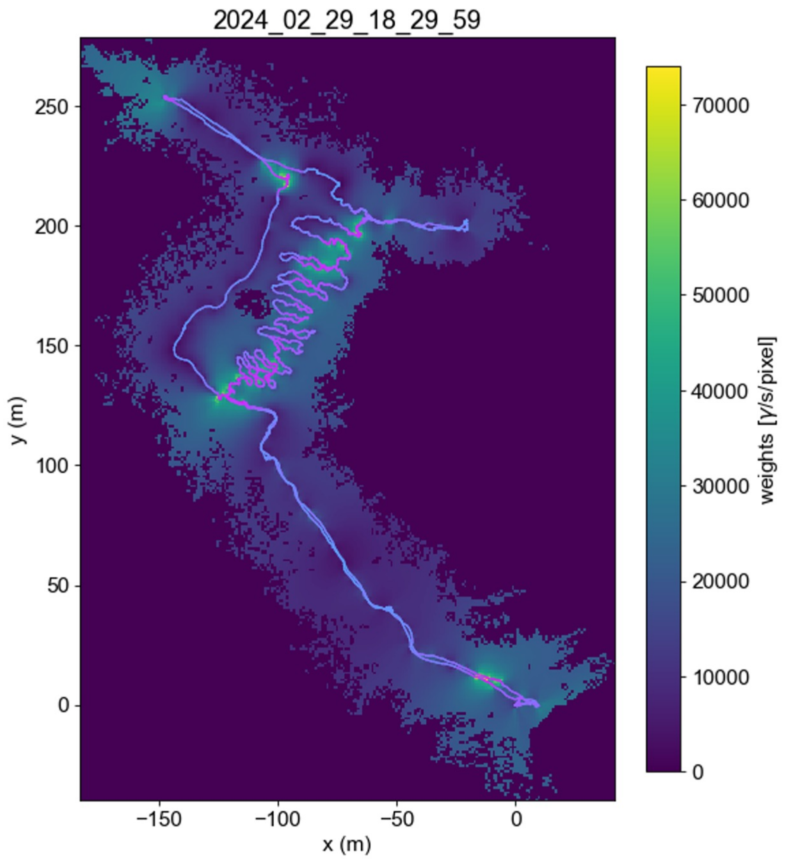

- Some pixels missing due to terrain complexity (e.g., Lidar view obstructed)
- Need to fill in missing pixels with estimated values before Rad map reconstruction

- Pixel value has low sensitivity if the measurement time near the pixel is short
- We can manually replace some pixels with inpainted value

Image inpainting by Deep Gaussian Markov Random Fields (DGMRF)

Ground Truth

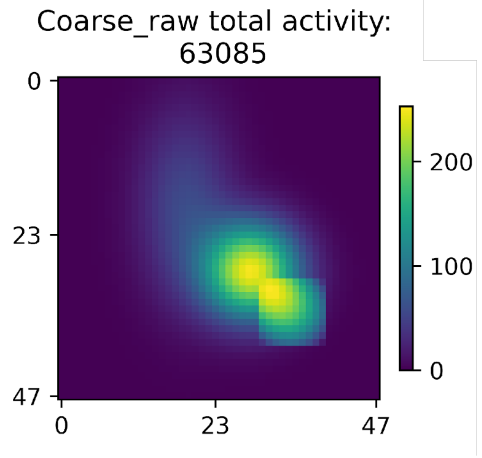

Manually drop some pixels

With missing pixels

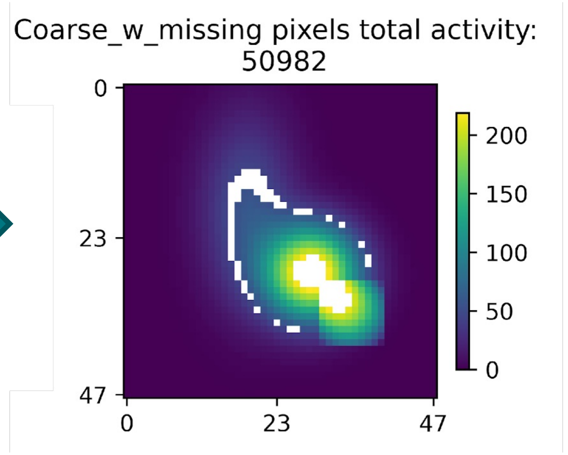

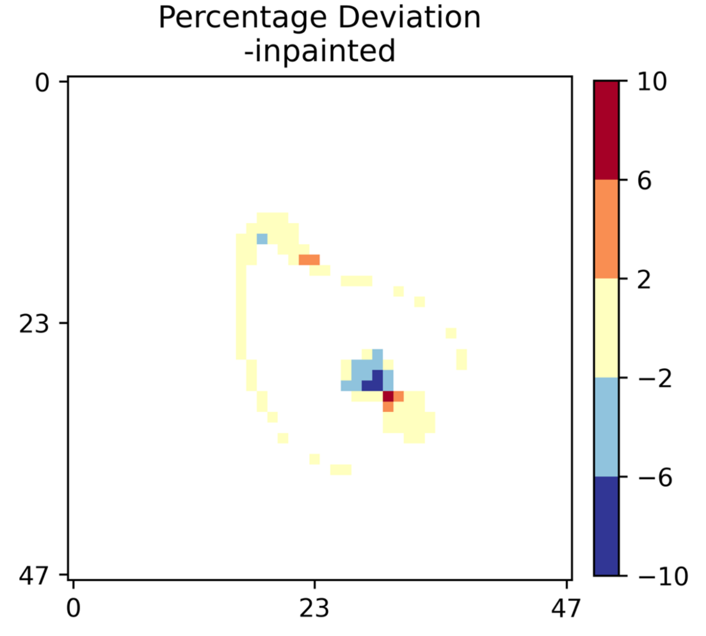

DGMRF model inpainting

PSNR: 47.6179
SSIM: 0.9989

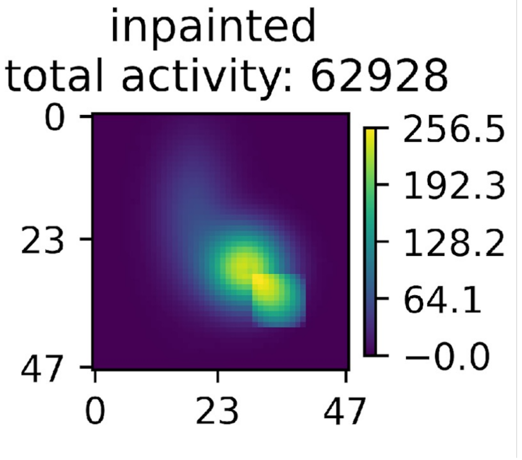

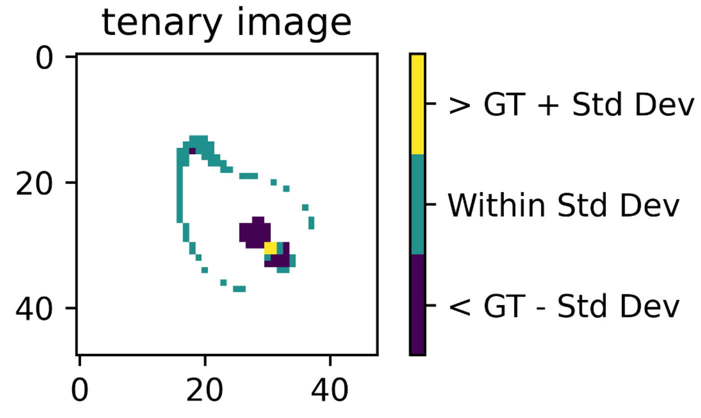

Radiation image reconstruction and uncertainty quantification

Bayesian inference for rad image reconstruction

$$\lambda = V \cdot w + b\, t$$

- w: radiation intensity
- V: system matrix
- b: background count rate
- t: measurement time
- λ: mean counts

- Measured counts x ~ Poisson(λ)
- Negative log likelihood

$$\ell(\mathbf{x}|\boldsymbol{\lambda}) = [\boldsymbol{\lambda} - \mathbf{x} \odot \log \boldsymbol{\lambda} + \log[\Gamma(\mathbf{x}+1)]]^{\mathrm{T}} \cdot \mathbf{1}$$

$$P(\theta|D) = \frac{P(D|\theta)P(\theta)}{P(D)}$$

- θ: w (radiation intensity) and b (background count rate)
- $P(\theta)$: assume w and b follow Gaussian distribution
- $P(D|\theta)$: likelihood

Use MCMC-based sampler to draw samples

- Traditional MCMC: slow at higher dimensions

MCLMC (Microcanonical Langevin Monte Carlo)

Jakob Robnik and Uroš Seljak. Microcanonical langevin monte carlo. *arXiv preprint arXiv:2303.18221*, 2023.

Synthetic data used for testing

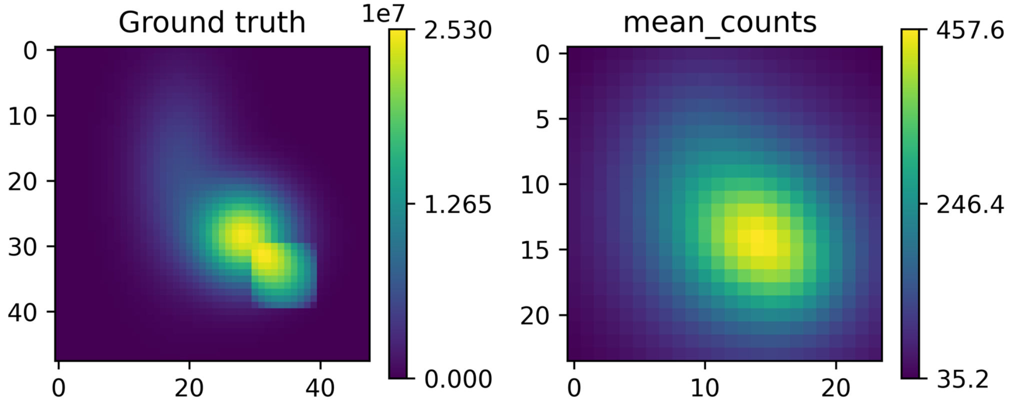

Preliminary results from MCLMC

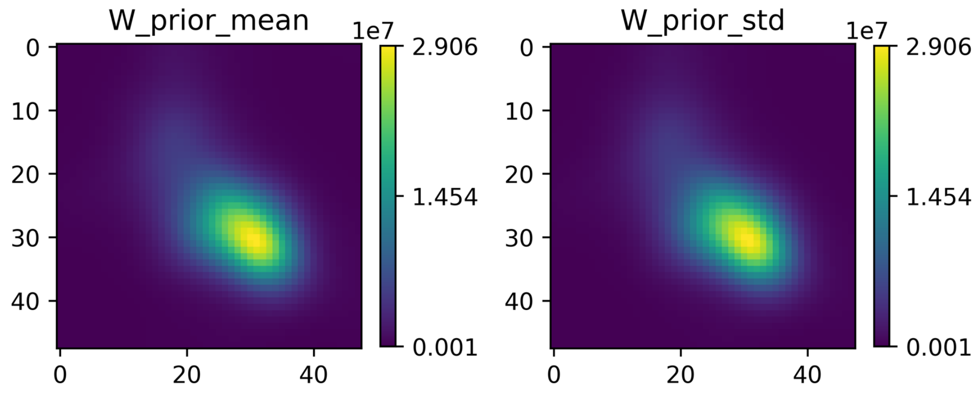

MLEM reconstruction used as prior for MCLMC sampling

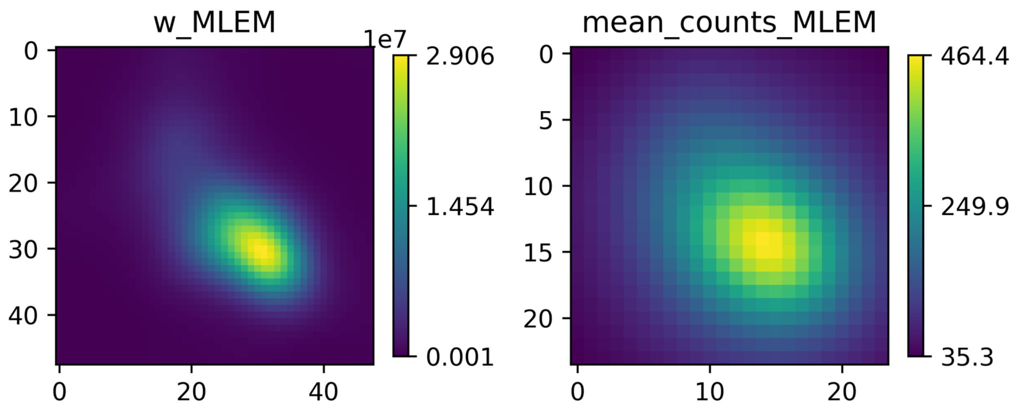

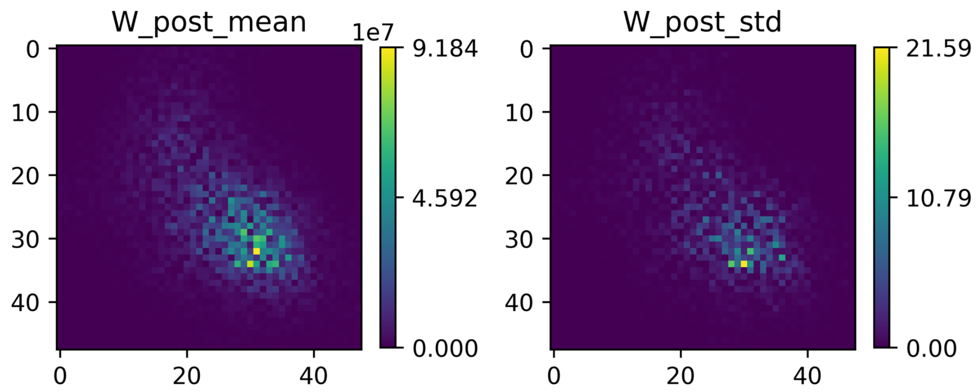

Acknowledgements

This work was performed under the auspices of the US Department of Energy by Lawrence Berkeley National Laboratory under Contract DE-AC02-05CH11231.

This work was funded by the DOE Office of Science (NP).

Backup slides

Rad image reconstruction principle

I measurements of radiation intensity $\mathbf{x}^{[I\times 1]} = [x_1, x_2, \ldots, x_I]^T$ made

- Unit of X_I: counts per unit integration time.
- I stands for discretized positions.

Intensity $\mathbf{x}^{[I\times 1]}$ follows Poisson distribution with mean $\boldsymbol{\lambda}^{[I\times 1]} = \mathbf{V}^{[I\times J]} \cdot \mathbf{W}^{[J\times 1]}$

- $\mathbf{V}^{[I\times J]}$: system matrix describes geometric and detector efficiency of I measurements relative to J image voxels (in units of inverse activity (Bq^{-1}))
- $\mathbf{W}^{[J\times 1]}$: intensities to be reconstructed (in units of activity (Bq) or emission rate (γ/s).

Measurements I independent of reconstructed image voxels J.
For same measurements, a high-fidelity reconstruction has more voxels (i.e., a larger J), so the system matrix $\mathbf{V}^{[I\times J]}$ has more entries.